An Introduction to the HydroGNSS GNSS Reflectometry Remote Sensing Mission

Martin J. Unwin ⑩, Nazzareno Pierdicca ⑩, *Senior Member, IEEE*, Estel Cardellach ⑩, *Senior Member, IEEE*, Kimmo Rautiainen, Giuseppe Foti ⑩, Paul Blunt, Leila Guerriero ⑩, *Member, IEEE*, Emanuele Santi ⑩, *Senior Member, IEEE*, and Michel Tossaint

Abstract—HydroGNSS (Hydrology using Global Navigation Satellite System reflections) has been selected as the second European Space Agency (ESA) Scout earth observation mission to demonstrate the capability of small satellites to deliver science. This article summarizes the case for HydroGNSS as developed during its system consolidation study. HydroGNSS is a high-value dual small satellite mission, which will prove new concepts and offer timely climate observations that supplement and complement the existing observations and are high in ESAs earth observation scientific priorities. The mission delivers the observations of four hydrological essential climate variables as defined by the global climate observing system using the new technique of GNSS reflectometry. These will cover the world's land mass to 25 km resolution, with a 15-day revisit. The variables are soil moisture, inundation or wetlands, freeze/thaw state, and above-ground biomass.

Index Terms—Global navigation satellite system (GNSS), global navigation satellite system reflectometry (GNSS-R), hydrology, remote sensing.

I. INTRODUCTION

A. HydroGNSS (Hydrology using Global Navigation Satellite System reflections)

COMPLEMENTING ESAs series of Earth Explorer research missions, Scout missions are a new element in ESAs Earth Observation FutureEO Programme. The intention is

Martin J. Unwin is with the Surrey Satellite Technology, Ltd., GU2 7YE Guildford, U.K. (e-mail: m.unwin@sstl.co.uk).

Nazzareno Pierdicca is with the Sapienza University of Rome, 00185 Rome, Italy (e-mail: nazzareno.pierdicca@uniroma1.it).

Estel Cardellach is with the Institute for Space Studies of Catalonia (IEEC), 08034 Barcelona, Spain, and also with Institute of Space Sciences (ICE-CSIC), 08193 Barcelona, Spain (e-mail: estel@ice.csic.es).

Kimmo Rautiainen is with the Finnish Meteorological Institute, 00560 Helsinki, Finland (e-mail: kimmo.rautiainen@fmi.fi).

Giuseppe Foti is with the National Oceanography Centre, SO14 3ZH Southampton, U.K. (e-mail: g.foti@noc.ac.uk).

Paul Blunt is with the University of Nottingham, Nottingham NG7 2RD, U.K. (e-mail: paul.blunt@nottingham.ac.uk).

Leila Guerriero is with the Tor Vergata University of Rome, 00133 Rome, Italy (e-mail: leila.guerriero@uniroma2.it).

Emanuele Santi is with the IFAC/CNR, 50019 Florence, Italy (e-mail: e.santi@ifac.cnr.it).

Michel Tossaint is with the European Space Agency, European Space Research and Technology Centre, 2201 AZ Noordwijk, The Netherlands (e-mail: michel.tossaint@esa.int).

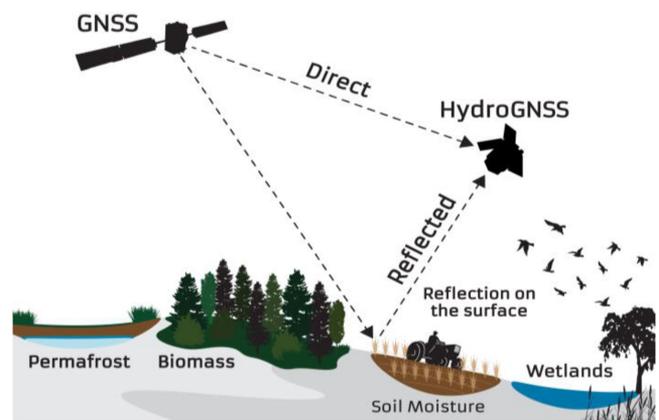Digital Object Identifier 10.1109/JSTARS.2021.3089550

Fig. 1. HydroGNSS uses a bistatic radar concept using GNSS-reflected signals for hydrological measurements, targeting soil moisture, freeze/thaw state over permafrost, AGB, soil moisture, and wetlands.

to demonstrate the capability of small satellites to deliver value-added science and implement a Scout mission, from kick-off to launch, within three years, and for a maximum of €30 million, covering the development of the space and ground segment, launch, and in-orbit commissioning.

HydroGNSS has been selected as the second Scout small satellite mission and is planned to be developed and launched before the end of 2024. Prior to selection, HydroGNSS was supported as one of the four candidate concepts to undergo a consolidation study, and the outputs of this study are summarized in this article. The study assumed two HydroGNSS satellites, although Scout funding is initially available for just a single satellite.

HydroGNSS uses GNSS reflectometry (GNSS-R) to target four hydrological essential climate variables (ECVs): soil moisture, wetlands/inundation, freeze/thaw state, and above-ground biomass (AGB) (see Fig. 1).

B. Importance of Hydrological Knowledge

Water is a natural resource vital to climate, weather, and life on earth, and unforeseen global variability in hydrology poses one of the greatest threats to the world's population [1]. Water manifests itself in or on the land in different ways, for example, moisture in the ground, wetlands and rivers, snow and ice, and

vegetation. The global knowledge of land water content and state is important in its different forms for many reasons.

1) Soil moisture knowledge is needed for weather forecast, hydrology, agriculture analysis, and wide-scale flood prediction.
2) The freeze/thaw state affects the surface radiation balance and the exchange rates of latent heat and carbon with the atmospheric boundary layer and acts as a tracer for subsurface permafrost behavior in high latitudes.
3) The AGB feeds into the understanding of carbon stock in forests and a sink in the carbon dioxide cycle and also has a coupling to biodiversity.
4) Wetlands are fragile water-dependent ecosystems, often hidden under forest canopies and that can also turn into sources of methane, while, elsewhere, an oversupply of water can lead to inundation and destructive flooding.

These four aspects of hydrology are identified as ECVs by the global climate observing system (GCOS) [2]. ECVs are defined in association with the United Nations Framework Convention on Climate Change, the Intergovernmental Panel on Climate Change, and the World Meteorological Organization in order to help understand and predict climate change to guide mitigation measures and to assess risks. Specific committees and programs address the need for the measurements of soil moisture (including freeze/thaw and inundation states), permafrost, and biomass, while wetlands are among the targets of the climate change initiative land cover and play a role as a primary source for greenhouse gases. Increasingly complex and accurate models are used to characterize and forecast hydrological processes: earth system models are used for climate and numerical weather prediction models for weather forecasting. These models have a requirement for hydrological observational data to be assimilated to ensure correspondence with the complexity of the real world.

C. GNSS-R Background

GNSSs, such as GPS and Galileo, comprise dozens of satellites in medium earth orbit that continually transmit low-power *L*-band microwave navigation signals toward the earth. These signals reflect back carrying the geophysical imprint of the surface. GNSS-R is a technique to collect these reflections, in this case, from low earth orbit (LEO) in order to sense the geophysical properties of the earth's surface [3].

Multiple reflections can be simultaneously collected by a single observatory in LEO; GPS and Galileo constellations alone offer more than 60 sources of *L*-band signals (see Fig. 2). Further sources are available from GLONASS, Beidou, NavIC, QZSS, and SBAS satellites, totaling over 130 once the constellations are complete.

Observations are made of the forward scattered reflections, i.e., implementing a bistatic radar geometry. The observations are usually captured in the form of delay Doppler maps (DDMs), where incoming signals are correlated with the on-board code replicas and integrated incoherently to give measurements from four simultaneous reflections (see Fig. 3).
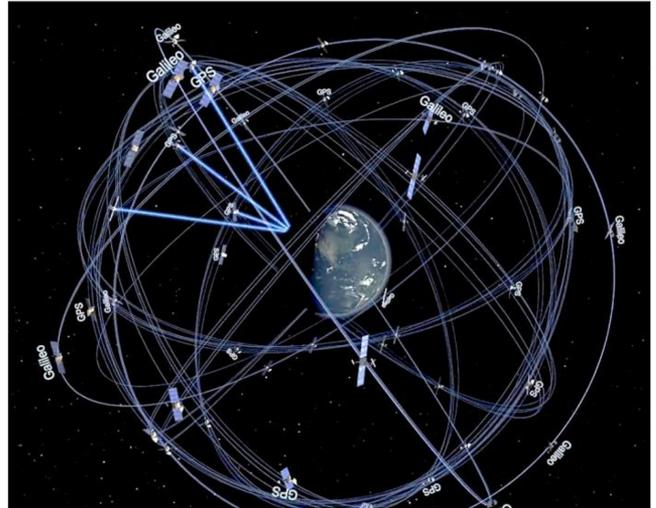

Fig. 2. GPS and Galileo satellites in medium earth orbit, amongst others, are available as signal sources for GNSS-R, and reflections are collected by a satellite in LEO [45].
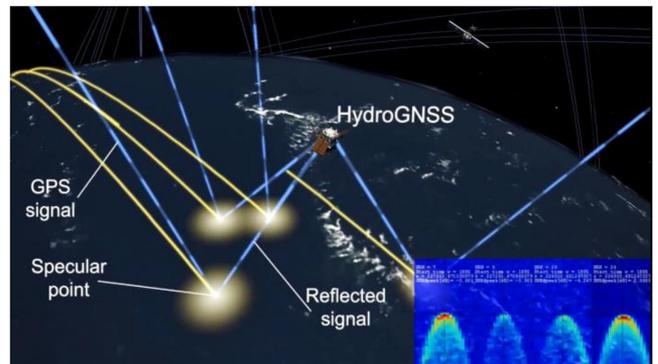

Fig. 3. Each HydroGNSS satellite collects multiple reflections from LEO. Yellow lines indicate the accumulated reflection tracks and results are represented as DDMs in the bottom right of the picture [45].

Surrey Satellite Technology, Ltd., (SSTL) has taken a leading role in GNSS-R developments since 2003, instigating the U.K.-DMC reflectometry experiment [4], TechDemoSAT-1 (TDS-1) sea state payload [5], and providing the instrumentation to the NASA eight-satellite CYGNSS constellation [6].

One original driver for spaceborne GNSS-R experimentation was for the scatterometric measurement of ocean winds and waves, and such applications have been well established as a result of the TDS-1 and CYGNSS satellite missions, e.g., [7]–[9]. Furthermore, as TDS-1 was in a polar orbit, it was able to show the potential of cryospheric applications, e.g., [10]–[12]. Ocean altimetry is a tantalizing target but achieving coherent carrier phase precision over a rough surface remains a technical challenge achieved only under certain conditions [29]. The potential of GNSS-R for land sensing was demonstrated by both TDS-1 and CYGNSS missions.

D. Land Sensing Using GNSS-R

Investigations on GNSS-R for land applications date back to the year 2000 [13]. Much work has been done using the

Fig. 4. Two campaigns using GNSS-R for land-sensing, (left) LEiMON investigated tower-based polarimetric GNSS-R as an agricultural tool [15], and (right) GRASS investigated airborne polarimetric GNSS-R measurement of soil moisture content and AGB [16].
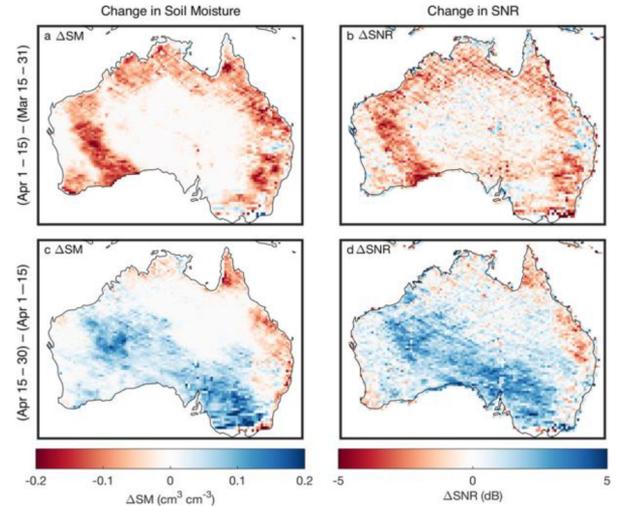

Fig. 5. Radiometer versus GNSS-R sensitivity to change in soil moisture during the first and second half of April 2017 over Australia. (a) and (c) Change in SMAP radiometer. (b) and (d) Change in CYGNSS GNSS-R SNR [22].

established ground-based GNSS receivers, for example, in the International GNSS Service network, for sensing land parameters, such as soil moisture and snow depth. These parameters are observable by quantifying the amplitude and phase effects caused by interference of reflected with direct GNSS signals through the same antenna [14].

Since around 2008, ground-based and airborne experiments demonstrated the sensitivity of reflected GNSS power to moisture, vegetation, and ice. Several ESA-funded projects (e.g., Fig. 4) made investigations using ground [15], airborne [16], and satellite GNSS-R measurements [17], and were accompanied by the corresponding models. These findings have fed into knowledge that enables the development of a case for a spaceborne hydrology mission, as discussed in Section II.

II. HydroGNSS Targets and Evidence

HydroGNSS aims at monitoring ECVs using GNSS-R techniques established by TDS-1 and CYGNSS, supplemented by dual-polarization and complex coherent channel measurements, as presented in Section IV, to support the separation of variables. The four ECV targets are discussed here as follows.

A. Soil Moisture

The capability of GNSS-R for deriving soil moisture measurements is based upon well-known mechanisms. Specular reflectivity is directly related to soil permittivity, which has good sensitivity at *L*-band GNSS sensing frequencies. Reflectivity is also inversely related to roughness and vegetation optical depth (VOD), which is the opposite of backscatter radar, a fact that further highlights the complementarity between GNSS-R and monostatic radar.

The sensitivity (in the range of 0.7–3.8 dB/10%) [15]–[17], [23], [24] is similar to that of the monostatic radar at similar electromagnetic bands and there is the potential of reaching a high resolution to the order of 2–7 km [17], significantly better than spaceborne microwave radiometers. The availability of dual-polarization GNSS measurements has been shown to help detangle soil moisture and roughness effects through the use of the polarization ratio; to some extent, roughness acts as a common factor, while soil moisture affects primarily left-hand

circular polarization [15], [16], [18], [19]. Nevertheless, ancillary data, such as VOD maps, are generally required to help separate the vegetation effects from soil moisture.

In addition to documented studies, at least one near-operational soil moisture product has been developed to date using GNSS-R data from CYGNSS [20], [21]. Fig. 5 demonstrates that the change in signal-to-noise ratio (SNR) from CYGNSS on the right is very similar to soil moisture maps from the NASA SMAP soil moisture satellite (see Fig. 5) [22].

B. Inundation/Wetlands

There is much evidence of GNSS-R capabilities in sensing inundation and wetlands even in the presence of vegetation [25], [26]. The concept has been proved using a spaceborne GNSS-R, as depicted in Fig. 6 , where a map from CYGNSS on the bottom is compared with the passive radiometer and active radar on SMAP [27], see also the articles presented in [22] and [25] for a general discussion.

The bistatic forward scattered signals are strong and coherent over the calm water and easy to be detected. The long GNSS *L*-band signal wavelengths ($\sim$19 cm) while partially attenuated by thick vegetation canopies have better penetration than the *C*-band radar and can show up strong reflecting surfaces. The ability for GNSS-R to sense water under forest canopies is unique and helps address limitations in the existing remote sensing measurements. The spatial resolution achievable improves as the reflection becomes coherent, approaching the resolution of the Fresnel zone, which is better than 1 km for *L*-band signals.

Furthermore, when surfaces are sufficiently flat, (e.g., rivers, lakes, and calm seas), strong coherent reflections allow the recovery of precise GNSS phase information, potentially enabling altimetry measurements [28], [29].
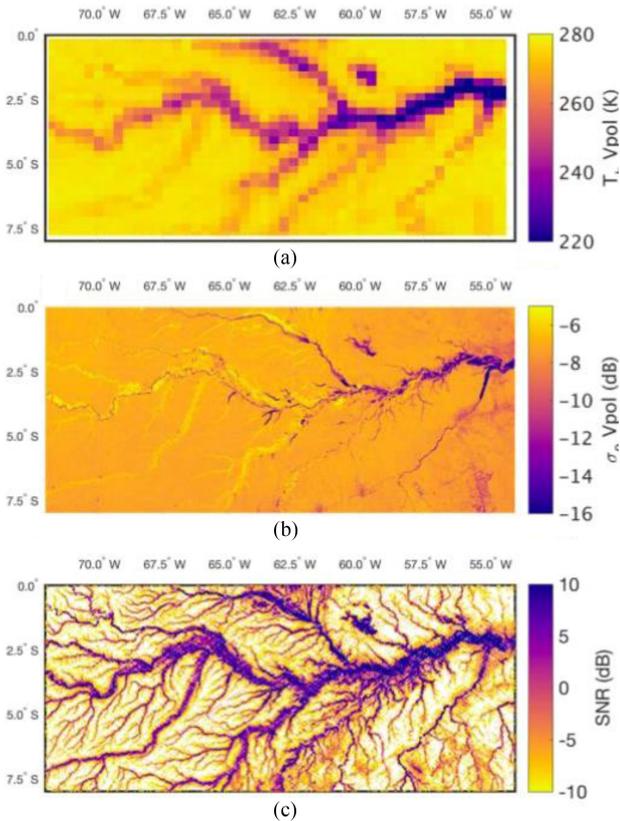
Fig. 6. Remote sensing of Amazon basin. (a) SMAP passive 36 km resolution brightness temperature, 2016. (b) SMAP active 3 km resolution data, 2015. (c) GNSS-R SNR from CYGNSS, 2017 [27].

C. Above-Ground Biomass

There is growing evidence that the AGB can also be retrieved from GNSS-R measurements. The mechanism is that the vegetation attenuates the soil-reflected signals due to the absorption and scattering phenomena. This generates an inverse correlation of the signal with respect to biomass, with a sensitivity that does not saturate as is usual for the L-band backscatter when biomass is greater than 150 t/ha [16], [30]–[33].

TDS-1 and CYGNSS GNSS-R data have been used to evaluate the sensitivity on both the local and global scale to VOD, AGB, and tree height. They are 16 dB/VOD, 0.05 dB $(t/ha)^{-1}$, and 0.7 dB/m, respectively. Fig. 7 provides an example of an AGB map derived from CYGNSS data using an artificial neural network (ANN) algorithm [33]. The algorithm was trained using a subset of pixels (1%) of an available pantropical AGB map. Fig. 8 provides the comparison between the retrieved and the reference AGB, and the statistical scores (correlation coefficient, root-mean-square error, and bias) refer to a test set containing the remaining 99% of pixels.

The measurement of reflections from areas with high biomass is a challenge due to the significant attenuation of the signals. A higher antenna gain and the availability of the coherent channel will improve the reception of weaker signals from the densest forests. A further challenge is the separation of AGB from the underlying surface soil characteristics, but polarimetric

measurements are anticipated to be correlated with AGB [16] and could provide additional independent information.

D. Soil Freeze/Thaw and Permafrost

Because of its depth, the state of permafrost cannot be measured directly by GNSS-R, but the active layer freeze/thaw state above can be sensed, and this provides a valuable input into permafrost models. Frozen soil has a much lower permittivity with respect to thawed soil; thus, surface-reflected signal diminishes in frozen conditions. The reflectivity measured is less directly related to the subsurface temperature than is the case for measurements made by microwave radiometers.

It was demonstrated in [34] that the increase of reflectivity between frozen and thawed states modeled according to the SMAP F/T product as observable in GNSS-R data. More recently (see Fig. 9), a high similarity between TDS-1 reflectivity monthly means (in green) and seasonal variability of SMAP FT products (in red) was observed when analyzing different land cover categories in Siberia [35]. With this capability, HydroGNSS can potentially help address any gap left when the ESA SMOS and NASA SMAP soil moisture satellites complete their missions.

III. HydroGNSS Mission Objectives

A. Objectives for HydroGNSS

Table I presents the ECV targets identified; HydroGNSS shall demonstrate the fulfillment of GCOS requirements for these ECVs by a suitable constellation of small satellites. The table summarizes the main requirements for level-2 specified after a survey of requirements from different entities, notably [2]. The spatial resolution can be fulfilled for three ECVs at the "breakthrough" level, while AGB is fulfilled at the "threshold" level. The spatial resolution of 25 km is typically achieved when signals are diffuse and shall be considered a threshold. The goal of 1 km refers to the exploitation of the complex signal over flatter surfaces where the reflected signal is more coherent. Temporal resolution is 15 days for two HydroGNSS satellites or 30 days for a single satellite but could be improved by increasing the number of satellites in the constellation.

The HydroGNSS satellites, in a near-polar orbit, will provide coverage over the whole world but with a denser coverage and a higher repeat rate, especially over the boreal climate regions. The standard data delivery target of 31 days is anticipated, but a preoperational fast service with 6 h of latency for dynamic soil moisture products is expected to be trialed later in the HydroGNSS mission.

B. HydroGNSS Secondary Objectives

The four land ECVs are the primary targets of HydroGNSS and take precedence over any other measurements and determine any optimization of operational settings. Nevertheless, the HydroGNSS mission is being scaled with the intention to allow continuous operation over all surfaces, as it is recognized that the same GNSS-R level-1 DDM measurements will be valuable for many other applications.
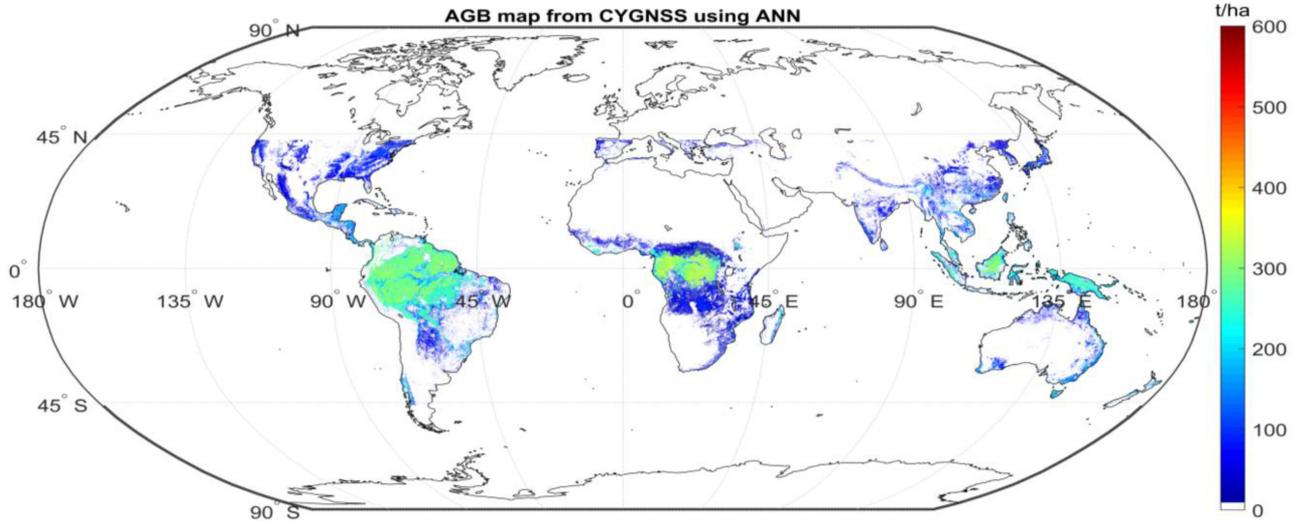
Fig. 7.   AGB estimated by ANN using CYGNSS data plotted on the global map. Results limited to within $+/-45°$ latitude due to the inclination of CYGNSS satellites [33]**.**
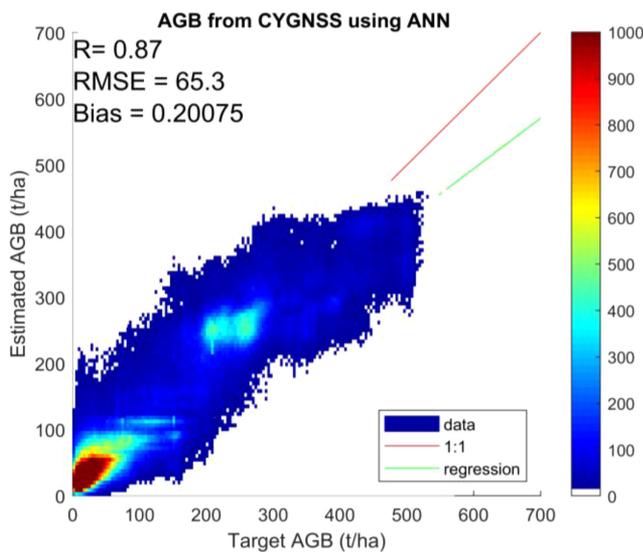

Fig. 8.   AGB estimated by ANN presented as a function of reference from a pantropical biomass map [33].
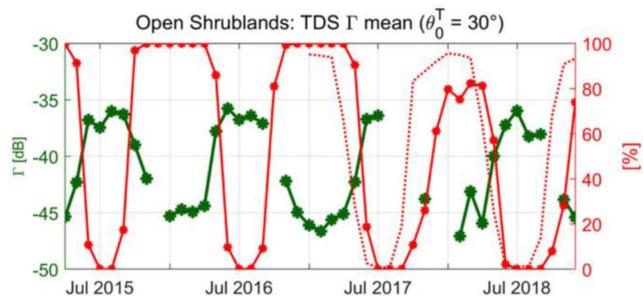

Fig. 9.   Time-series analysis of SMAP FT fraction (solid red curve, right axis) and percentage of frozen pixels (dotted red curve, right axis) versus TDS-1 seasonal reflectivity (green, left axis) over Siberian permafrost shrublands [35].

As a result of TDS-1 and CYGNSS, GNSS-R has been established as a technique for measuring ocean winds. The accuracy of independent algorithms has been shown to be in the order of 2 m/s for winds up to 20 m/s [see Fig. 10(a)] [7], [36], [37], with the benefit of careful calibration. Uniquely, GNSS-R is also able to retrieve measurements through the most severe cyclones, although winds are measured less accurately ($>15\%$) due to the saturation of parameters [8], [38]. Sea ice can also be measured with sea ice extent validated to 98% accuracy and sea ice concentration validated with $<9\%$ error. A study has also showed that TDS-1 measurements can be useful in measuring the Greenland ice sheet melting fraction [see Fig. 10(b)] [10], [12].

With the ability to capture coherent reflections, GNSS carrier phase measurements are enabled, unlocking the potential of accurate polar ice height altimetry and even for measuring sea ice thickness [11].

It is planned that level-2 products for ocean wind speed and ice extent will be made available from HydroGNSS based on the measurements and algorithms validated on TDS-1 but remain a lower mission priority than the land ECV level-2 products.

IV. HydroGNSS Products

A. Innovations

To maintain compatibility with previous successful TDS-1 and CYGNSS missions, HydroGNSS will offer established GNSS-R measurements based on incoherent DDMs from GPS C/A code at GPS L1 frequency (1.575 GHz) at 1 Hz. In addition to these, HydroGNSS will offer innovative GNSS-R measurements that have not been available previously (see Fig. 11).

1) Galileo Signals – DDMs from Galileo E1 will be generated, offering double the coverage from the same antenna field of view. The Galileo codes are longer (in common with other future GNSS signals), which means that less
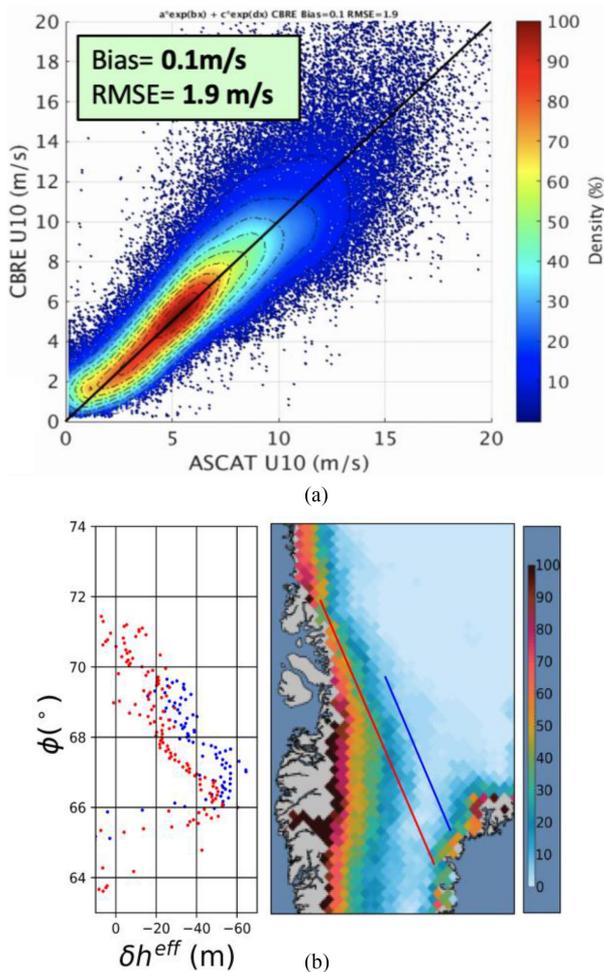
(a)

(b)

Fig. 10.   Secondary applications anticipated from HydroGNSS. (a) Ocean wind speed retrieved from TDS-1 GNSS-R measurements versus winds from ASCAT 2017 [36]. (b) Effective height of Greenland ice against latitude derived using two TDS-1 tracks in January 2015 compared against Greenland cumulative melt days (right) from NSIDC, showing apparent correlation [12].
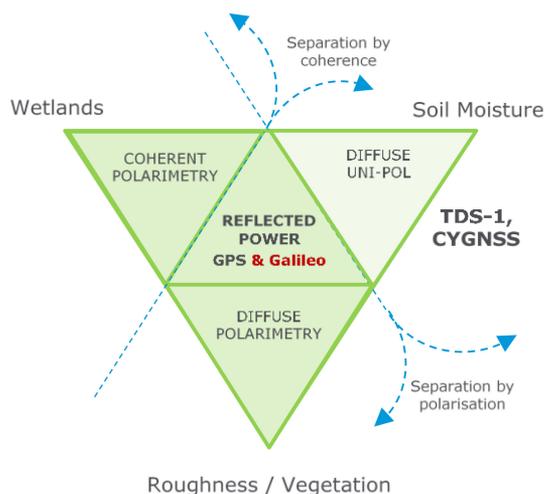

Fig. 11.   New measurements on HydroGNSS compared with TDS-1 and CYGNSS. Top right of the triangle shows the extent of measurement from TDS-1 and CYGNSS, restricted to diffuse, unipolar measurements from GPS. Top left and bottom triangles are added with a coherent channel, polarimetric, and Galileo measurements.

TABLE I
HydroGNSS Level-2 Product Requirements

ECV	Units	Horiz. Resln	Uncertainty	Temp Resln
Surface Soil Moisture	m^3/m^3	25 km (1 km)	0.04	15 (30) days
Surface Inundation	Flag	25 km (1 km)	90%[a]	15 (30) days
Freeze/Thaw State	Flag	25 km (1 km)	90%[a]	15 (30) days
Above Ground Biomass	t/ha	25 km (1 km)	< 20% error[b]	15 (30) days

[a] i.e., 90% classification accuracy; [b] or 10 t/ha when AGB < 50 t/ha.

TABLE II
HydroGNSS Level-0 Measurement Set ($\sqrt{}/\sqrt{}$ Indicates New)

Level 0b	GPS L1 LHCP	GPS L1 RHCP	Galileo E1 LHCP	Galileo E1 RHCP
Non-coherent DDMs	✓	✓✓	✓✓	✓✓
Coherent Channel	✓✓	✓✓	✓✓	✓✓
Black Body	✓	✓✓	Same	Same
Metadata	Incl. settings, temperatures, GNSS positions, etc.			

Level 0a	L1/E1 LHCP	L1/E1 RHCP	L5/E5 LHCP	L5/E5 RHCP
Sampled Data	✓	✓✓	✓✓	✓✓
(LHCP / RHCP mean Left and Right Hand Circular Polarised)				

cross-correlation noise is to be expected from the unwanted GNSS signals.

2) Polarization – DDMs will be collected from both left- and right-hand circular polarizations of the antenna. The ratio of the two polarizations (RR/LR) can help separate soil roughness effects from soil moisture and also plays a role in the separation of biomass from ground reflections.

3) Coherent complex channel – A channel is added to each DDM (of both polarizations) that captures the coherent amplitude and phase of the signal at a higher rate. This allows further separation of flat surfaces, accesses higher resolution than the incoherent DDMs, and gives the flexibility to implement longer integrations for weaker signals and allowing focusing techniques. It also enables precise altimetric measurements under certain conditions.

4) Second frequency – The ability to sample signals prior to processing onboard will be used to capture both L1/E1 signals and the wide bandwidth L5/E5 GNSS signals. Models suggest that the wideband signals reflected may be weak but, if proved viable, the rewards could be a higher resolution from these signals. As the instrument is reprogrammable, it is planned to exercise E5/L5 on-board processing schemes at a later stage of the mission, even once in orbit.

All these new measurements will be backed up by simulations to help understand and validate level-2 product generation.

Table II presents the measurements in tabular form with a single tick indicating measurements previously available on TDS-1 and CYGNSS and a double tick for measurements new to HydroGNSS. In addition to the dual-polarized DDMs and
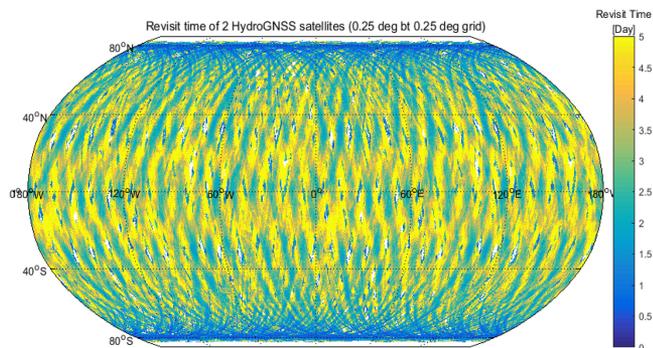
Fig. 12. Simulated revisit time of two HydroGNSS satellites over the globe using $0.25° \times 0.25°$ cells over a period of 30 days; the mean revisit time at any point on the globe is less than 3 days, and near the poles, the density of coverage is higher and revisit time lower.
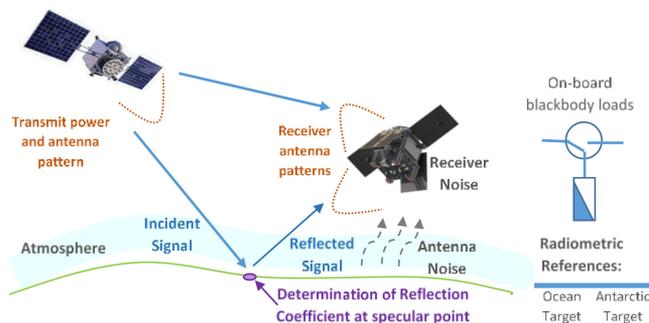

Fig. 13. Factors affecting the measurement of reflection coefficient at specular point, including direct powers, antenna patterns, and antenna noise. Corrections will be developed using of on-board blackbody loads as well as external targets over ocean and ice.

coherent channels, data will be collected from blackbody loads. The metadata will include many additional parameters required for level-1 corrections. The raw sampled data collections will be scheduled, including dual-polarization and dual-frequency configurations for specific target reflection investigations.

B. Measurement Coverage

In keeping with the scope of the Scout opportunity, HydroGNSS will initially be comprised of one or two satellites in a near-polar LEO but with a view toward a larger future constellation. To achieve consistent coverage, two satellites could be launched together and phased apart by 180°. By selecting a commonly used orbit, 550 km 10:30 A.M. longitude time at ascending node (LTAN) sunsynchronous, it makes low-cost rideshare more likely and enables passive re-entry at the end of the mission. In this orbit, simulations of two satellites indicate a coverage over the earth in 15 days (84%), assuming a resolution of $0.25° \times 0.25°$ (equivalent to 27 km $\times$ 27 km at the equator), and an antenna field of view of +/-35°. The revisit time is illustrated in Fig. 12; the mean revisit time in this orbit at any point on the globe is calculated as less than 3 days. If only one HydroGNSS satellite is available, the earth is covered in 30 days with a global mean revisit time of just under 4 days.

C. Calibration Approach

Achieving good absolute calibrated performance is an important requirement of HydroGNSS. Prelaunch tests will be carried out to measure instrument noise figure, receiver gain, and antenna patterns. Once in orbit, the collection of spacecraft information, such as attitude knowledge, low-noise amplifier (LNA) temperature, and direct signal powers, will be required. Experience from TDS-1 and CYGNSS missions will be applied to HydroGNSS [37], [39], and the use of ocean-reflected signals will play a role in correcting the receiver and transmitter terms for application over the land. A diagram showing the factors affecting the calibration is given in Fig. 13.

1) The antenna noise will be corrected by blackbody loads noise routed to the nadir and zenith LNA as well as using ground target, e.g., Antarctic dome-C.

2) The receiving antenna correction terms are a function of azimuth and off-pointing and can be determined from the long-term data over the ocean.
3) The GNSS transmit powers and antenna patterns (for each GNSS satellite) can also be determined through the long-term data over the ocean plus other methods and, in particular, the use of the direct signal measurement to monitor temporal changes in the transmitter power and/or the use of other GNSS observatories (from ground or space) providing accurate transmitter power.

New calibration challenges include the following.
1) Calibration of the Galileo signals—further information may be available from Galileo authorities or other observatories.
2) Calibration of the dual-polarization signals (polarimetric calibration) of the coherent signals and intercalibration with multiple GNSS-R satellites.

D. Level-2 Algorithms and Validation

The baseline level-2 ECV products will be generated using consolidated algorithms based on the literature and past studies, with an aim to later incorporate findings from future studies. The empirical change detection [20], [40] and ANN-based algorithms [24] have been exploited for soil moisture and, after appropriate scaling, compared against SMAP, SMOS, and *in situ* data (e.g., Fig. 14). Freeze/thaw discrimination will be based on the change detection methods [35], while the inundation flag will exploit the coherence [29]. Biomass retrieval is foreseen to make use of the neural networks [33]. Ancillary data, such as land cover and VOD maps, are likely to be required.

There are a number of resources available for validation, notably SMOS and SMAP missions, while they continue to operate. The International soil moisture network collates many measurements, and models, such as the ECMWF ERA-5, provide a source of reference data. The biomass mission and the GlobBiomass database will allow the comparison of AGB measurements with HydroGNSS.

The exploitation of the new HydroGNSS features in the algorithm (polarimetry, coherence, and Galileo signals) will be investigated by simulation. A target interaction simulator for GNSS-R reflections over land has been developed and validated
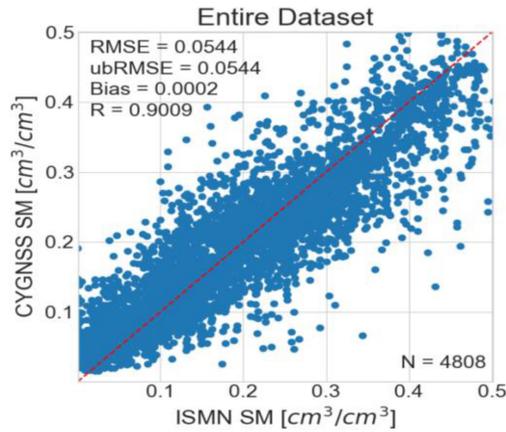
Fig. 14.   Example of ANN CYGNSS soil moisture retrievals tested against international soil moisture network sites over 2017 and 2018 [24].

Fig. 15.   Data flow of the level-1 component of the end-to-end simulator implementation for the HydroGNSS mission. Green, red, and blue boxes represent the geometric, sensor, and target interaction subsystems, respectively, of the entire level-1 E2E simulator.
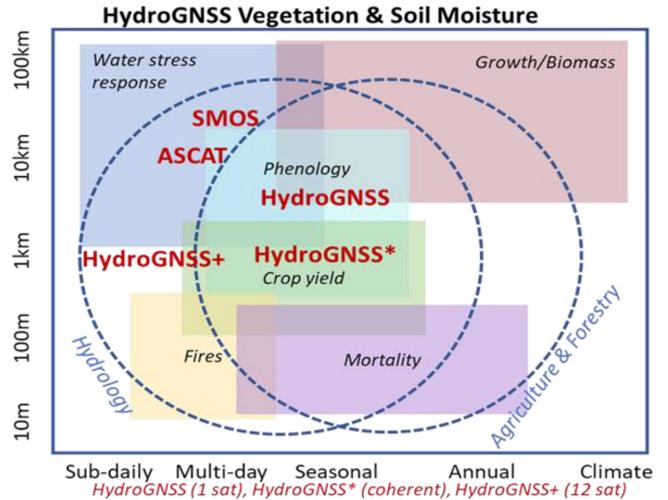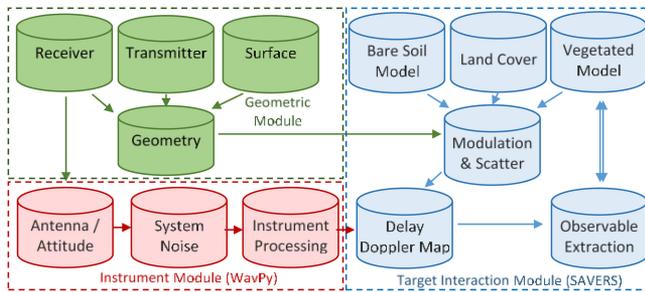

Fig. 16.   Temporal and spatial resolution plot showing anticipated HydroGNSS capability with respect to land sensing needs. HydroGNSS* indicates the spatial resolution improvement due to the new coherent channel and HydroGNSS+ indicates the improved temporal resolution from adding satellites.

for ground, airborne, and spaceborne applications by a team composed by Sapienza and Tor Vergata Universities of Rome. The simulator is called the soil and vegetation reflection simulator [19], [41]. The level-1 waveform simulation in Python, developed by the Institute of Space Sciences, IEEC-CSIC in Barcelona, is an open-source library that provides a set of object-oriented classes dedicated to each of the different elements that characterize a GNSS-R scenario [42]. Its main focus up until now has been on ocean and ice applications but can be applied to land. These two simulators will form the target interaction and instrument modules of the end-to-end simulator, as shown in Fig. 15.

E. Complementarity With Other Missions

Aside from other GNSS-R demonstration missions, CYGNSS, and FSSCat, the functionally closest missions to HydroGNSS (targeting global soil moisture measurements) are the L-band radiometry missions SMOS and SMAP but, by 2024, these missions may have completed as they are well past their design life, with successor satellites some years away. Scatterometer and SAR satellites, such as MetOp-1 ASCAT, and Sentinel-3 operate at higher frequency C-band; their measurements are valued for hydrology but do not penetrate vegetation and so cannot replace SMOS and SMAP.

Copernicus high priority missions CIMR (radiometry) and ROSE-L (SAR) are currently progressing, although funding still needs to be confirmed, and these will not be ready until at least 2026. SMOS-HR is a CNES-sponsored follow-on to SMOS, offering 10 km resolution and advanced radio frequency interference mitigation techniques, and has recently entered Phase A of its mission. Other missions targeting water cycle with L-band include the Chinese WCOM [43] and the TWRS [44] satellites.

HydroGNSS, therefore, offers to provide some continuity between the existing and future L-band missions. As it uses a different technique to others, it will remain valuable as a complementary data source once the new Copernicus missions and SMOS-HR soil moisture products become available.

The ESA Earth Explorer Biomass mission is due for launch late in 2022. It will provide exceptional data on forests but has coverage gaps and low temporal sampling, so HydroGNSS can offer complementary observations.

Fig. 16 illustrates the temporal and spatial resolutions and how they relate to certain hydrological applications. Resolution ranges covered for instance by SMOS and ASCAT aboard MetOp are indicated in the range of a few tens of kilometers and multiday temporal resolution.

A single conventional GNSS-R-based satellite would have slightly better resolution than SMOS and ASCAT but worse revisit, still supporting, for instance, some phenology studies. Coherent HydroGNSS measurements (denoted by an asterisk) can improve spatial resolution and become useful for crop yield estimation. A constellation of HydroGNSS satellites (with the plus symbol) would increase the temporal resolution with enhanced features and could fulfill an even wider range of application requirements in the hydrological domain. A constellation of satellites of the scale of CIMR or ROSE-L ($>$700 kg) is simply not practical, while the small size and low cost of GNSS-R
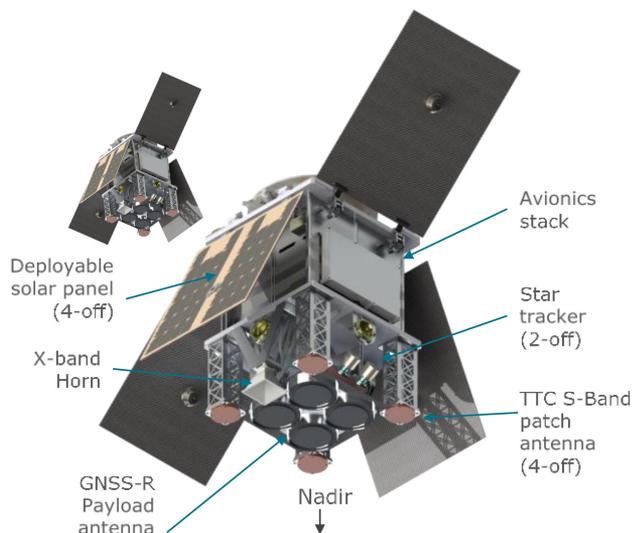
Fig. 17. Two HydroGNSS satellites showing an in-orbit configuration with deployed solar panels. The GNSS-R nadir antenna is visible, comprising of four patch excited cup antennas capable of dual frequency and dual polarization.
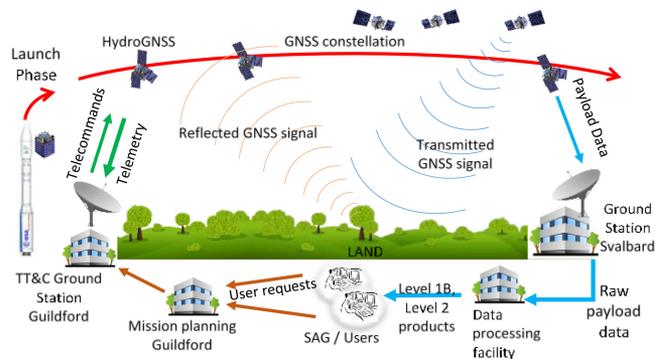

Fig. 18. Mission architecture and operations overview for HydroGNSS, including launch, telemetry, and telecommand via Guildford, operational reflectometry collection, and data download via a ground station at Svalbard, data processing and delivery of level-1 and 2 products to users.

Fig. 19. HydroGNSS timeline from launch and early operations to platform and payload commissioning, operational phase, potential life extension, and end-of-life activities.

missions mean a constellation could be envisaged at a budget compatible with future earth observation programs.

V. MISSION ARCHITECTURE

The mission architecture comprises the satellite payload, satellite platform, control and downlink ground segment, and the payload data ground segment (PDGS).

A. Platform and Launch

The platform that has been selected for HydroGNSS is the "SSTL-21," which is the smallest family member of the "SSTL-micro" platform. This is a highly capable platform but small enough to maintain the low cost of a future constellation (see Fig. 17). It has dual redundant avionics, three-axis attitude stabilization, *X*-band-link supporting high data downlinks, up to 160 MB/s, and a propulsion system with up to 30 m/s delta-v. It is 45 cm × 45 cm ×70 cm in size and has a mass of 40 kg.

In particular, this platform offers HydroGNSS mission 100% duty cycle, star camera attitude accuracy, and a high data throughput, which will serve to raise the quality of the science data. These capabilities would be difficult to match using a smaller platform, such as a Cubesat.

In terms of system budgets, the SSTL-21 offers good margins for the HydroGNSS mission. The orbit average power is 41.5 W, assuming 100% payload operations and 5% of the time for downlinks. As the platform generates 56 W, this gives a healthy 26% margin. The TTC and payload links both have positive margins. It is estimated that the mission requires 13.6 m/s out of the satellite's capacity of 30 m/s delta-v of propulsion; for phasing orbits and for collision avoidance. The satellite will naturally re-enter within 25 years due to the low altitude, meeting the deorbit requirements, but the spare propellant could be used to speed this up or alternatively to extend the mission life.

A common sunsynchronous orbit (10:30 LTAN, 550 km) has been selected to ensure a timely and good value launch. The GNSS-R payload operates night and day and is not bound to a particular hour angle or ground repeat track, so it could be put into a number of similar near-polar orbits. The baseline assumption is a rideshare on ESAs Vega launch vehicle, but the satellites are compatible with several other options, which should be an alternative launch that need to be considered.

B. Operations and Data Processing

Fig. 18 shows the mission architecture for HydroGNSS, and Fig. 19 shows the operational timeline. After launch, the satellite(s) will be commissioned using the Guildford ground station and, if present, the second satellite phased 180° apart from the first after a tip-off from the launch vehicle. Following the platform and payload commissioning, the payloads will be operated continuously for a 3-year lifetime with the potential of a 2-year life extension. The data will be downloaded via Svalbard, which means that the data can potentially be processed in the PDGS and disseminated to users rapidly. At the end of the mission, the satellites will be allowed to deorbit.

The payload data processing scheme evolves from MERRByS that has been delivering processed TDS-1 GNSS-R data to users since not long after its launch in 2014. Fig. 20 shows the different levels of data planned from the HydroGNSS satellite. Payload operations are not complex, as the payloads will usually be generating L0B data comprising DDMs on-board the satellite continuously, but the collections of raw sampled data will be scheduled over specified targets.

Level-0A and level-0B data are reformatted and concurrent metadata is prepared, and level-1 data disseminated to users.
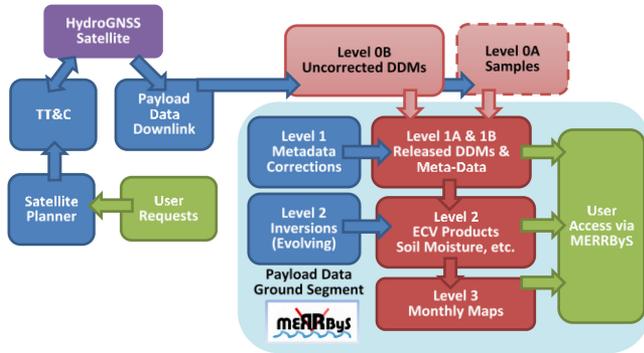
Fig. 20.   HydroGNSS operational ground segment, PDGS, data product levels, and user data access.
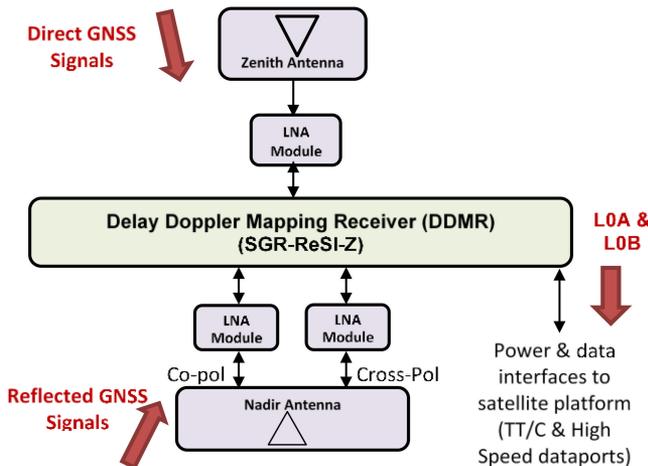

Fig. 21.   HydroGNSS payload overview, comprising nadir and zenith antennas, LNAs, and a DDMR (also known as SGR-ReSI-Z). The DDMR continually processes GNSS reflections into DDMs as level-0B products.

The level-2 processing will generate the ECV products, such as soil moisture, which again are disseminated. It is expected that the level-2 processors will evolve with time as new GNSS-R measurements are better understood, and new algorithms are validated.

Level-3 will comprise periodic maps of the products—either monthly or more often.

C. HydroGNSS Payload

The HydroGNSS Payload (see Fig. 21) is an evolution from the SGR-ReSI remote sensing instrument flown on TDS-1 and CYGNSS.

The central unit is a delay doppler mapping receiver (DDMR). There is one zenith antenna tracking direct GNSS signals, and the nadir antenna collecting reflected signals and processing them into DDMs. The LNAs contain blackbody loads that give reference noise measurements. Once collected, the level-0A and level-0B data are sent to the data recorder in the satellite platform for later download.

A similar medium high-gain antenna requirement as on TDS-1 and CYGNSS is being adopted. This will allow the targeting of weak signals under vegetation without losing the wide beamwidth needed to collect multiple reflections. This antenna

must support dual polarization and dual frequency (L1/E1, L5/E5), so a fixed array of 2×2 dual-patch excited cup elements has been selected. This gives a gain of around 14 dBi at L1 with good cross-polar performance at both frequencies and takes a physical area of about 32 cm $\times$ 32 cm on the spacecraft. The LNA uses a similar approach to those on CYGNSS, including a cavity filter, temperature sensor, load switch, and test ports.

Two quad channel front ends are used to collect signals from the nadir and zenith channels. A Zynq processor with a field programmable gate array is responsible for tracking the GNSS signals and processing the DDMs. The zoom transform correlator is implemented in VHDL (high-level hardware description language) within the Zynq processor and is driven by the application software running on the Zynq.

The key instrument performance parameters have been defined that affect level-1 and level-2 results, and include GNSS sensitivity, stability, and the performance of the signal processing approach used.

For HydroGNSS, the new measurements determine the need for the new front ends and processor architecture. Tests have been undertaken that demonstrate that the front ends are suitable for dual-polarization measurements.

SSTL has access to a testbed in-orbit on DoT-1, an 18 kg engineering satellite that was launched in August 2019. With sponsorship from ESA, it has been possible to test the new processing architecture in orbit on the Zynq processor within DoT-1 and generate DDMs in orbit. While the DoT-1 satellite mission has its limitations, it acts as an important stepping stone for HydroGNSS.

D. Small Satellite Approach

HydroGNSS will be built using the small satellite approach and timely schedule that SSTL has used for the past 35 years and 60+ satellites. Most of the equipment on the HydroGNSS platform have a high technology readiness level and heritage due to the use in orbit on other satellites, such as the Vesta Cubesat, DoT-1 microsatellite, and the Theos-2 satellite currently in build. Other equipment is being procured with a qualified status.

The greatest attention is being given to the less mature subsystems, including the power system, data recorder, and the instrument itself. Where possible, technology is being adopted from previous missions. Design and development verification plans are prepared for each unit, and engineering qualification models are being used for qualification testing. To save time and costs, where appropriate, requirement verification is being performed at the spacecraft level during engineering verification testing. SSTL is working with ESA on the tailoring of space standards (ECSS) to ensure the correct level of quality assurance for this small mission.

VI. CONCLUSION

HydroGNSS is a small satellite concept that uses GNSS-R to address internationally agreed ECVs using an evidence-based methodology: soil moisture, inundation, freeze/thaw state, and AGB. In comparison with other established passive hydrological missions, HydroGNSS offers better spatial resolution at L-band for an order less in cost, with an affordable route for increasing coverage.

The mission is both unique and complementary. The forward scatter measurements are different to those from other sensors. The mission is timely as it addresses a potential gap in *L*-band measurements. In terms of geography, it is global but with excellent coverage over polar regions and provides measurements where the ESA biomass mission cannot. The HydroGNSS measurements penetrate vegetation and so are excellent augmentation to *C*-band radar measurements. It is a low-cost approach that can be supplemented and sustained with lower budgets than normally associated with such missions.

GNSS-R is low risk but offers high gains. It is founded on TDS-1 and CYGNSS capabilities but offering world first new measurements. Although its main targets are over the land, around 70% of the time, the HydroGNSS satellites will be collecting DDMs over oceans and ice, and many users are able to exploit these secondary measurements. The dual satellites are optimally sized at 40 kg, offering excellent power density, attitude, and downlink capabilities while still making use of the small satellite approach.

HydroGNSS will be implemented by a strong industrial and academic team that will address both theory and practice, and the team is backed up by an established GNSS-R user community ready to provide support and ensure results that are fully exploited as a new methodology for remote sensing of the planet.

REFERENCES

[1] A. Jenkins *et al.*, "HydroSOS—The hydrological status and outlook system," *WMO Bull.*, vol. 69, no. 1, pp. 14–19, 2020.

[2] "Essential climate variables factsheets," Global Climate Observ. Syst., Geneva, Switzerland. [Online]. Accessed: Apr. 2021. Available: https://gcos.wmo.int/en/essential-climate-variables

[3] V. U. Zavorotny, S. Gleason, E. Cardellach, and A. Camps, "Tutorial on remote sensing using GNSS bistatic radar of opportunity," *IEEE Geosci. Remote Sens. Mag.,* vol. 2, no. 4, pp. 8–45, Dec. 2014.

[4] S. Gleason *et al.*, "Detection and processing of bistatically reflected GPS signals from low earth orbit for the purpose of ocean remote sensing," *IEEE Trans. Geosci. Remote Sens.*, vol. 43, no. 6, pp. 1229–1241, Jun. 2005.

[5] M. Unwin, P. Jales, J. Tye, C. Gommenginger, G. Foti, and J. Rosello, "Spaceborne GNSS-reflectometry on techdemosat-1: Early mission operations and exploitation," *IEEE J. Sel. Topics Appl. Earth Observ. Remote Sens.*, vol. 9, no. 10, pp. 4525–4539, Oct. 2016.

[6] C. Ruf *et al.*, "CYGNSS: Enabling the future of hurricane prediction," *IEEE Geosci. Remote Sens. Mag.*, vol. 1, no. 2, pp. 52–67, Jun. 2013.

[7] G. Foti *et al.*, "Spaceborne GNSS reflectometry for ocean winds: First results from the U.K. techdemosat-1 mission," *Geophys. Res. Lett.*, vol. 42, no. 13, pp. 5435–5441, 2015.

[8] M. P. Clarizia and C. S. Ruf, "Statistical derivation of wind speeds from CYGNSS data," *IEEE Trans. Geosci. Remote Sens.*, vol. 58, no. 6, pp. 3955–3964, Jun. 2020.

[9] E. Cardellach, Y. Nan, W. Li, R. Padullés, S. Ribó, and A. Rius, "Variational retrievals of high winds using uncalibrated CyGNSS observables," *Remote Sens.*, vol. 12, 2020, Art. no. 3930.

[10] W. Li, E. Cardellach, F. Fabra, S. Ribo, and A. Rius, "Measuring Greenland ice sheet melt using spaceborne GNSS reflectometry from TechDemoSat-1," *Geophys. Res. Lett.*, vol. 47, no. 2, 2020, Art. no. e2019GL086477.

[11] W. Li, E. Cardellach, F. Fabra, A. Rius, S. Ribó, and M. Martín-Neira, "First spaceborne phase altimetry over sea ice using techdemosat-1 GNSS-R signals," *Geophys. Res. Lett.*, vol. 44, pp. 8369–8376, 2017.

[12] A. Rius, E. Cardellach, F. Fabra, W. Li, S. Ribó, and M. Hernández-Pajares, "Feasibility of GNSS-R ice sheet altimetry in Greenland using TDS-1," *Remote Sens.*, vol. 9, 2017, Art. no. 742.

[13] D. Masters, V. Zavorotny, S. Katzberg, and W. Emery, "GPS signal scattering from land for moisture content determination," in *Proc. IEEE Int. Geosci. Remote Sens. Symp.*, 2000, pp. 3090–3092.

[14] K. M. Larson, E. E. Small, E. D. Gutmann, A. L. Bilich, J. J. Braun, and V. U. Zavorotny, "Use of GPS receivers as a soil moisture network for water cycle studies," *Geophys. Res. Lett.*, vol. 35, no. 24, Dec. 2008, Art. no. L24405.

[15] A. Egido *et al.*, "Global navigation satellite systems reflectometry as a remote sensing tool for agriculture," *Remote Sens.*, vol. 4, pp. 2356–2372, 2012.

[16] A. Egido *et al.*, "Airborne GNSS-R polarimetric measurements for soil moisture and above ground biomass estimation," *IEEE J. Sel. Topics Appl. Earth Observ. Remote Sens.*, vol. 7, no. 5, pp. 1522–1532, May 2014.

[17] A. Camps *et al.*, "Potential of spaceborne GNSS-R for land applications," ESA/ESTEC, Noordwijk, The Netherlands, Tech. Rep. 4000120299/17/NL/AF/hh, GLA-FR/1, 2020.

[18] H. Carreno-Luengo, S. Lowe, C. Zuffada, S. Esterhuizen, and S. Oveisgharan, "Spaceborne GNSS-R from the SMAP mission: First assessment of polarimetric scatterometry over land and cryosphere," *Remote Sens.*, vol. 9, no. 4, 2017, Art. no. 362.

[19] L. Dente, L. Guerriero, D. Comite, and N. Pierdicca, "Space-borne GNSS-R signal over a complex topography: Modelling and validation," *IEEE J. Sel. Topics Appl. Earth Observ. Remote Sens.*, vol. 13, pp. 1218–1233, 2020.

[20] C. C. Chew and E. E. Small, "Soil moisture sensing using spaceborne GNSS reflections: Comparison of CYGNSS reflectivity to SMAP soil moisture," *Geophys. Res. Lett.*, vol. 45, no. 9, pp. 4049–4057, 2018.

[21] C. Chew and E. Small, "Description of the UCAR/CU soil moisture product," *Remote Sens.*, vol. 12, no. 10, 2020, Art. no. 1558.

[22] C. S. Ruf *et al.*, "A new paradigm in earth environmental monitoring with the CYGNSS small satellite constellation," *Sci. Rep.*, vol. 8, no. 1, Jun. 2018, Art. no. 8782.

[23] A. Camps, M. Vall-Llossera, H. Park, G. Portal, and L. Rossato, "Sensitivity of TDS-1 GNSS-R reflectivity to soil moisture: Global and regional differences and impact of different spatial scales," *Remote Sens.*, vol. 10, no. 11, 2018, Art. no. 1856.

[24] O. Eroglu, M. Kurum, D. Boyd, and A. C. Gurbuz, "High spatio-temporal resolution CYGNSS soil moisture estimates using artificial neural networks," *Remote Sens.*, vol. 11, 2019, Art. no. 2272.

[25] S. V. Nghiem *et al.*, "Wetland monitoring with global navigation satellite system reflectometry," *Earth Space Sci.*, vol. 4, pp. 16–39, 2017.

[26] N. Rodriguez-Alvarez, E. Podest, K. Jensen, and K. C. McDonald, "Classifying inundation in a tropical wetlands complex with GNSS-R," *Remote Sens.*, vol. 11, no. 9, 2019, Art. no. 1053.

[27] C. Chew, "A modest proposal? Using 'free' L-band signals to sense changes in soil moisture and inundation," Jet Propul. Lab. Climate Center Seminar, Pasadena, CA, USA, 2017.

[28] W. Li, E. Cardellach, F. Fabra, S. Ribo, and A. Rius, "Lake level and surface topography measured with spaceborne GNSS-Reflectometry from CYGNSS mission: Example for the Lake Qinghai," *Geophys. Res. Lett.*, vol. 45, pp. 13 332–13 341, 2018.

[29] E. Cardellach *et al.*, "First precise spaceborne sea surface altimetry with GNSS reflected signals," *IEEE J. Sel. Topics Appl. Earth Observ. Remote Sens.*, vol. 13, pp. 102–112, 2020.

[30] M. Zribi *et al.*, "Potential applications of GNSS-R observations over agricultural areas: Results from the GLORI airborne campaign," *Remote Sens.*, vol. 10, no. 8, 2018, Art. no. 1245.

[31] E. Santi *et al.*, "Remote sensing of forest biomass using GNSS reflectometry," *J. Sel. Topics Appl. Earth Observ. Remote Sens.*, vol. 13, pp. 2351–2368, 2020.

[32] H. Carreno-Luengo, G. Luzi, and M. Crosetto, "Above-ground biomass retrieval over tropical forests: A novel GNSS-R approach with CYGNSS," *Remote Sens.*, vol. 12, 2020, Art. no. 1368.

[33] E. Santi *et al.*, "Forest biomass monitoring at local and global scale by using GNSS reflectometry techniques," *IGARSS 2019 - 2019 IEEE International Geosci. Remote Sens. Symp.*, 2019, pp. 8680-8683, doi: 10.1109/IGARSS.2019.8899140.

[34] C. Chew *et al.*, "SMAP radar receiver measures land surface freeze/thaw state through capture of forward-scattered L-band signals," *Remote Sens. Environ.*, vol. 198, pp. 333–344, Sep. 2017.

[35] D. Comite, L. Cenci, A. Colliander, and N. Pierdicca, "Monitoring freeze-thaw state by means of GNSS reflectometry: An analysis of TechDemoSat-1 data," *IEEE J. Sel. Topics Appl. Earth Observ. Remote Sens.*, vol. 13, pp. 2996–3005, 2020.

[36] G. Foti, C. Gommenginger, M. Unwin, P. Jales, and J. Rosello, "Preliminary analyses and early validation of calibrated spaceborne GNSS-R data from the U.K. techdemosat-1 mission for ocean wind retrieval," *Ocean Scatterometry*, GNSS+R2017, Ann Arbor, MI, USA, May 24, 2017. [Online]. Available: https://www.gnssr2017.org/images/Wednesday_afternoon/GNSS+R2017_WE_PM_1_Foti_TDS-1.pdf

[37] M. L. Hammond, G. Foti, C. Gommenginger, and M. Srokosz, "Temporal variability of GNSS-reflectometry ocean wind speed retrieval performance during the U.K. techdemosat-1 mission," *Remote Sens. Environ.,* vol. 242, Jun. 2020, Art. no. 111744, doi: 10.1016/j.rse.2020.111744.

[38] G. Foti, C. Gommenginger, and M. Srokosz, "First spaceborne GNSS-reflectometry observations of hurricanes from the U.K. techdemosat-1 mission," *Geophys. Res. Lett.,* vol. 44, no. 24, pp. 12358–12366, 2017.

[39] S. Gleason, C. S. Ruf, A. J. O'Brien, and D. S. McKague, "The CYGNSS level 1 calibration algorithm and error analysis based on on-orbit measurements," *IEEE J. Sel. Topics Appl. Earth Observ. Remote Sens.,* vol. 12, no. 1, pp. 37–49, Jan. 2019.

[40] M. P. Clarizia, N. Pierdicca, F. Costantini, and N. Floury, "Analysis of CYGNSS data for soil moisture retrieval," *IEEE J. Sel. Topics Appl. Earth Observ. Remote Sens.*, vol. 12, no. 7, pp. 2227–2235, Jul. 2019.

[41] N. Pierdicca, L. Guerriero, R. Giusto, M. Brogioni, and A. Egido, "Savers: A simulator of GNSS reflections from bare and vegetated soils," *IEEE Trans. Geosci. Remote Sens.,* vol. 52, no. 10, pp. 6542–6554, Oct. 2014.

[42] F. Fabra, E. Cardellach, W. Li, and A. Rius, "WAVPY: A GNSS-R open source software library for data analysis and simulation," in *Proc. Int. Geosci. Remote Sens. Symp.*, 2017, pp. 4125–4128.

[43] J. Shi *et al.*, "WCOM: The science scenario and objectives of a global water cycle observation mission," in *Proc. IEEE Geosci. Remote Sens. Symp.*, 2014, pp. 3646–3649.

[44] T. Zhao *et al.*, "Soil moisture experiment in the Luan river supporting new satellite mission opportunities," *Remote Sens. Environ.,* vol. 240, 2020, Art. no. 111680.

[45] HydroGNSS Smallsat Mission Animation, SSTLTV, YouTube, 2020. [Online]. Available: https://youtu.be/30pemNtyBVA

Martin J. Unwin received the Ph.D. degree in spaceborne Global Positioning System (GPS) from the University of Surrey, Guildford, U.K, in 1995.

He initiated and led the GPS team with Surrey Satellite Technology, Ltd. (SSTL), designing the SGR-20 space GPS receiver which flew on UoSAT-12 and Proba-1. The GPS team succeeded in demonstrating autonomous orbit control, attitude determination in orbit, operation of GPS above the GPS constellation, and the development of GPS reflectometry instruments on U.K.-DMC, TDS-1, and CYGNSS satellites. He had involvement in GIOVE-A and Galileo FOC projects from the beginning. He is currently a Principal Engineer with SSTL, Guildford, U.K., and is working on the development of newer generation global navigation satellite system receivers for remote sensing.

Nazzareno Pierdicca (Senior Member, IEEE) received the Laurea (Doctorate) degree in electronic engineering (*cum laude*) from the University La Sapienza of Rome, Rome, Italy, in 1981.

From 1978 to 1982, he was with the Italian Agency for Alternative Energy, and from 1982 to 1990, with Remote Sensing Division, Telespazio, Rome. In November 1990, he joined the Department of Information Engineering, Electronics, and Telecommunications, Sapienza University of Rome, Rome. He is currently a Full Professor of remote sensing, antenna, and electromagnetic fields with the Faculty of Engineering, Sapienza University of Rome, Rome, Italy. His research interests include electromagnetic scattering and emission models for sea and bare soil surfaces and their inversion, microwave radiometry of the atmosphere, radar land applications, and bistatic radar.

Dr. Pierdicca is a past Chairman of the Geoscience and Remote Sensing Society Central Italy Chapter.

Estel Cardellach (Senior Member, IEEE) received the Ph.D. degree in physics from the Polytechnic University of Catalonia, Barcelona, Spain, in 2002.

She has been involved in scientific applications of global navigation satellite systems (GNSS) for remote sensing of the earth, such as the extraction of geophysical information of the GNSS-reflected signals, radio occultation, and geodetic techniques. She was a Postdoctor with NASA/Jet Propulsion Laboratory, Pasadena, CA, USA, in 2003, and the Harvard Smithsonian Center for Astrophysics, Cambridge, MA, USA, in 2004. Since 2005, she has been with the Institute of Space Sciences (ICE-CSIC/IEEC), Barcelona, Spain. She was a Co-Chair of the Science Advisory Group of the European Space Agency's (ESAs) GEROS-ISS mission, and a Co-Principal Investigator of the G-TERN proposal, in response to ESA EE9 mission call. She is currently a Principal Investigator of the spaceborne experiment radio-occultation and heavy precipitation aboard the PAZ low earth orbiter.

Kimmo Rautiainen received the D.Sc.(tech.) degree from the Helsinki University of Technology (TKK), Espoo, Finland, in 2018.

He was a Research Scientist with the TKK Laboratory of Space Technology and the TKK Department of Radio Science and Engineering, where he focused on microwave radiometer systems with an emphasis on interferometric radiometers. Since 2010, he has been a Scientist with Arctic Research and the Earth Observation Research Units, Finnish Meteorological Institute, Helsinki, Finland, where he was involved in the development of retrieval algorithms for passive microwave remote sensing, with a focus on cryosphere applications.

Giuseppe Foti received the M.Eng. degree in electronics engineering from the University of Catania, Catania, Italy, in 2000, and the M.Sc. degree in oceanography from the University of Southampton, Southampton, U.K., in 2013.

In 2001, he joined Communication Systems Section, European Space Agency, Noordwijk, The Netherlands, where he was involved in the field of spread-spectrum techniques for packet access in broadband satellite systems. From 2003 to 2010, he was a Patent Examiner with the Principal Directorate of Telecommunications, European Patent Office, Rijswijk, The Netherlands. In 2013, he joined Satellite Oceanography Section, National Oceanography Centre, Southampton, U.K., where he is currently a Research Scientist. His research interest focuses on remote sensing of the oceans, with special emphasis on techniques using signals of opportunity.

Paul Blunt received the Ph.D. degree in advanced global navigation satellite system (GNSS) receiver design from the University of Surrey, Guildford, U.K., in 2007.

He has been a Research Scientist with Electronics and Signal Processing Laboratory, École Polytechnique Fédérale de Lausanne, Lausanne, Switzerland, and is currently an Associate Professor of GNSS and communications engineering with the University of Nottingham, Nottingham, U.K. His research is performed with Nottingham Geospatial Institute and he teaches the Department of Electrical and Electronic Engineering. His research interests include all aspects of GNSS signal acquisition and tracking, scientific applications of GNSS, and interference mitigation. He has a wide-ranging experience in industry and academia. His main field of work and research is GNSS receiver design and he has designed receivers for space, military, mass market, and scientific applications.

Leila Guerriero (Member, IEEE) received the Laurea degree in physics from the Sapienza University of Rome, Rome, Italy, in 1986, and the Ph.D. degree in electromagnetism from the Tor Vergata University of Rome, Rome, Italy, in 1991.

Since 1994, she has been a Permanent Researcher with the Tor Vergata University of Rome, where she is currently an Associate Professor holding the courses on earth satellite observation and on geoinformation. She has participated in several international projects, including the European Space Research (ESA) projects soil moisture and ocean salinity satellite, the development of SAR inversion algorithms for land applications, the use of bistatic microwave measurements for earth observation, and the SAOCOM-CS bistatic imaging, radiometry, and interferometry over land. Finally, she has been involved in the modeling of global navigation satellite system reflectometry (GNSS-R) signals for ESA projects and in the European FP7 and H2020 Programs. Her research interests include modeling microwave scattering and emissivity from agricultural and forested areas.

Dr. Guerriero is a member of the Permanent Steering Scientific Committee of MicroRad. She is the Secretary of the Geoscience and Remote Sensing Society North-Central Italy Chapter.

Michel Tossaint received the M.Sc. degree in aerospace engineering from the Delft University of Technology, Delft, The Netherlands, in 1997.

He is a System Engineer with Earth Observation - Future Mission Division, European Space Research and Technology Centre, European Space Agency (ESA), Noordwijk, The Netherlands. He joined Space Systems Department, Dutch NLR, in 1998. In 2001, he joined ESA working on navigation-related topics, such as EGNOS design and validation, Galileo experimentation with GIOVE satellites, and Geoscience and Remote Sensing Society evolutions in general. Since 2008, he has been a Navigation Technical Officer in the Galileo project and evolution program working on intersatellite links and Galileo second-generation design.

Emanuele Santi (Senior Member, IEEE) received the M.S. degree in electronic engineering from the University of Florence, Florence, Italy, in 1997, and the Ph.D. degree in earth's remote-sensing techniques from the University of Basilicata, Potenza, Italy, in 2005.

Since 1998, he has been a Researcher with Microwave Remote Sensing Group, Institute of Applied Physics, National Research Council, Florence, Italy. He is currently involved in many national and international projects funded by the Italian Space Agency, European Community, European Space Agency, and Japanese Aerospace Exploration Agency, acting as a Team Leader, a WP Leader, and a Co-Investigator. He has authored or coauthored 158 articles, published in ISI journals and books and conference proceedings (source Scopus). His research interests include the development and validation of models and statistical inversion algorithms for estimating the geophysical parameters of soil, sea, snow, and vegetation from microwave emission and scattering.

Dr. Santi was a recipient of the IEEE Geoscience and Remote Sensing Society J-STARS Prize Paper Award in 2018 for the best paper published in the *JSTARS Journal* in 2017. He is a member of the "Centro di Telerilevamento a Microonde" (Microwave Remote Sensing Center). He is also the Conference Chair of the SPIE Europe Remote Sensing Conference RS-106.